APPLICABLE NONLINEAR ANALYSIS
Volume 4 (2027), No. 1, 1–9
DOI:https://doi.org/10.69829/apna-027-0401-ta01
Tulipa Opera Scholarum

A REFINED FORMULATION AND RIGOROUS ANALYSIS OF AN INVERSE FREE BOUNDARY PROBLEM IN MODELING DUCTAL CARCINOMA IN SITU

HENG LI[1,*], DER-CHEN CHANG[2], AND YONGZHI XU[3]

[1] *Division of Science Mathematics and Technology, Governors State University, University Park, IL 60484, USA*
[2] *Department of Mathematics and Statistics, Georgetown University, Washington D.C. 20057, USA and Graduate Institute of Business Administration, Fu Jen Catholic University, New Taipei City 242, Taiwan, ROC*
[3] *Department of Mathematics, University of Louisville, Louisville, KY 40292, United States*

Abstract. We revisit a mathematical model for ductal carcinoma in situ (DCIS) growth described by a free boundary problem. Specifically, we address an algebraic oversight in the fixed-domain transformation of an inverse problem aimed at recovering the tumor growth potential from terminal biopsy data. We derive the refined parabolic partial differential equation step-by-step, establish the exact boundary evaluation, and prove the uniqueness of the reconstructed potential. Furthermore, we construct the clinical data function via a spectral eigenfunction expansion, casting the inverse problem as a first-kind Fredholm integral equation to analyze its exact existence via Picard's criterion. Demonstrating the severe ill-posedness of the problem under clinical noise, we propose a Tikhonov regularization scheme. We explicitly connect these functional analytic proofs to the physical reality of the breast duct, providing rigorous guarantees for the existence of a unique regularized biological solution. Finally, we present comprehensive computational simulations, validating the algorithm's robustness and optimal convergence against noisy synthetic clinical data.

Keywords. Inverse free boundary problem, ductal carcinoma in situ, Tikhonov regularization, Fredholm integral equation, Picard's criterion, spectral method.

© Applicable Nonlinear Analysis

1. Introduction

Ductal carcinoma in situ (DCIS) is a non-invasive breast cancer confined to the breast ducts. Mathematical modeling of DCIS using free boundary problems has become a powerful tool for understanding tumor growth dynamics [1, 4, 5, 6, 9, 10, 11, 12, 13]. In these models, the tumor boundary evolves over time based on the local concentration of nutrients, which diffuses through the tissue and is consumed by the proliferating cancer cells.

While the forward problem—predicting tumor growth given known biological parameters—has been extensively studied, the clinical reality is often the reverse. Clinicians typically observe the tumor at a specific moment in time via an incisional biopsy and must infer its underlying growth potential. This motivates the formulation of inverse problems. In a foundational study, Xu and Gilbert formulated several inverse problems based on different clinical diagnostic procedures [13].

Our focus is on the problem denoted as **IP1(b)** in [13]: determining the spatially dependent nutrient consumption rate, $\lambda(x)$, assuming that the tumor concentration profile and its rate of change are known only at a terminal time $t = T$ from a single incisional biopsy.

*Corresponding author.
E-mail address: hli@govst.edu (H. Li), chang@georgetown.edu (D.-C. Chang), and yongzhi.xu@louisville.edu (Y. Xu)
2020 Mathematics Subject Classification: 35R30, 35R35, 92C50, 65M32.
Accepted: May 01, 2026.

While Xu and Gilbert proposed an algorithmic construction and Tikhonov regularization scheme for IP1(b) in [13], the mathematical foundation for this specific inverse problem can be further strengthened and refined in two key areas:

label=(1) **Domain transformation dynamics:** When converting the moving boundary problem to a fixed domain, the resulting advection term mapping the boundary velocity must scale as $s'(t)/s(t)$. The original derivation contained an algebraic oversight, scaling this term by $s^2(t)$, which alters the characteristics of the parabolic PDE.

lbbel=(2) **Existence of the inverse solution:** Establishing uniqueness for IP1(b) is highly beneficial, but it is completed by constructing the formal Fredholm operator, analyzing the existence of a solution for the original exact problem, and proving the existence of a regularized solution in the appropriate functional spaces using the direct method of the calculus of variations [2, 7, 8].

In this paper, we refine the fixed-domain transformation of the 1D DCIS model, derive the exact difference equations, construct the right-hand data function using a corrected spectral expansion, and provide a rigorous functional analytic proof of existence, uniqueness, and convergence for the regularized tumor growth potential $\lambda(x)$. We conclude with numerical simulations demonstrating the efficacy of our algorithm.

2. Refined Formulation of the Direct Problem

One typical type of DCIS is the solid type, where cancer cells completely fill the affected breast duct. We describe this by a one-dimensional model. We assume the tumor to be within the interval $[-s(t)/2, s(t)/2]$ at each time t. We model tumor growth using a dimensionless nutrient concentration $c(y,t)$ which satisfies a reaction-diffusion equation. The model is given by:

$$\frac{\partial c}{\partial t} = \frac{\partial^2 c}{\partial y^2} - \lambda(y)c, \quad \text{in } B(t), \quad t > 0, \tag{2.1}$$

$$c(-s(t)/2, t) = c_1, \quad t > 0, \tag{2.2}$$

$$c(s(t)/2, t) = c_1, \quad t > 0, \tag{2.3}$$

$$c(y, 0) = c_0(y), \quad \text{in } B(0), \tag{2.4}$$

$$\frac{\partial s}{\partial t} = \mu \int_{-s(t)/2}^{s(t)/2} (c - \tilde{c}) dy, \quad s(0) = s_0, \tag{2.5}$$

where $B(t) = \{y \mid -s(t)/2 < y < s(t)/2\}$. Here $\lambda(y)c(y,t)$ is the nutrient consumption rate at location y, c_1 is the constant duct boundary supply, and $\tilde{c}$ is the critical viability threshold.

We change the variable $y \in [-s(t)/2, s(t)/2]$ to a fixed normalized domain $x \in [0,1]$ by setting $y = s(t)x - s(t)/2$. Let us define the shifted concentration:

$$v(x,t) = c\left(s(t)x - \frac{s(t)}{2}, t\right) - c_1, \quad 0 \le x \le 1, \quad t \ge 0. \tag{2.6}$$

Applying the chain rule, we have the partial derivatives of c in terms of v:

$$c_y = \frac{1}{s(t)} v_x, \tag{2.7}$$

$$c_{yy} = \frac{1}{s^2(t)} v_{xx}, \tag{2.8}$$

$$c_t = v_t - c_y \frac{\partial y}{\partial t} = v_t - \frac{1}{s(t)} v_x \left(s'(t)x - \frac{s'(t)}{2}\right) = v_t - \frac{s'(t)}{s(t)} \left(x - \frac{1}{2}\right) v_x. \tag{2.9}$$

From the free boundary condition (2.5), we have:

$$s'(t) = \mu \int_0^1 [v(\xi,t) + c_1 - \tilde{c}]\, s(t) d\xi \implies s(t) = s_0 e^{\mu \int_0^t \int_0^1 [v(\xi,\tau)+c_1-\tilde{c}] d\xi d\tau}. \tag{2.10}$$

Substituting the derivatives into (2.1), the free boundary problem is converted to an initial-boundary value problem of a nonlinear parabolic equation on a fixed domain:

$$\frac{\partial v}{\partial t} - \frac{1}{s^2(t)}\frac{\partial^2 v}{\partial x^2} - \frac{s'(t)}{s(t)}\left(x - \frac{1}{2}\right)\frac{\partial v}{\partial x} + \lambda(x)v = -\lambda(x)c_1, \quad 0 < x < 1, \quad t > 0, \tag{2.11}$$

$$v(0,t) = 0, \tag{2.12}$$

$$v(1,t) = 0, \tag{2.13}$$

$$v(x,0) = c_0(x) - c_1, \tag{2.14}$$

$$s(t) = s_0 e^{\mu \int_0^t \int_0^1 [v(\xi,\tau)+c_1-\tilde{c}] d\xi d\tau}. \tag{2.15}$$

Remark 2.1. In the foundational formulation [4], an algebraic oversight in the chain rule application placed $s^2(t)$ in the denominator of the advection term instead of $s(t)$. Equation (2.9) demonstrates the refined application of the chain rule. Addressing this is an important refinement, as it strictly aligns the mathematical PDE with the physical internal fluid velocity field induced by the boundary expansion of the DCIS tumor.

3. Uniqueness of The Inverse Problem

To properly frame the uniqueness proof, we must first rigorously define the clinical inverse problem denoted as **IP1(b)** in the literature [13]. This problem models an incisional biopsy performed at a terminal time T, from which both the spatial state and the dynamic rate of change of the tumor are observed.

3.1. **Statement of inverse problem IP1(b):**

Assume that the tumor concentration $c(y,t)$ and its free boundary $s(t)$ satisfy the moving-boundary direct problem given by equations (2.1)–(2.5). At a specific terminal time $t = T$, clinical diagnostics provide the following specific measurements:

label=(1) The terminal physical size of the tumor:

$$s(T) = s_T \tag{3.1}$$

lbbel=(2) The spatial profile of the nutrient concentration across the tumor at the terminal time:

$$c(y,T) = c_T(y), \quad \text{for } y \in \left[-\frac{s_T}{2}, \frac{s_T}{2}\right] \tag{3.2}$$

lcbel=(3) An integrated measurement of the instantaneous rate of change of the concentration, filtered through a known clinical biopsy weight function $\omega(y,\xi)$ over a parameter space $\xi \in \mathcal{O}$:

$$\int_{-s_T/2}^{s_T/2} c_t(y,T)\omega(y,\xi)dy = W(\xi), \quad \text{for } \xi \in \mathcal{O} \tag{3.3}$$

The objective of **IP1(b)** is to reconstruct the spatially dependent tumor consumption rate $\lambda(y)$ for all $y \in [-s_T/2, s_T/2]$ using the measured data $\{s_T, c_T(y), W(\xi)\}$.

To analyze this mathematically, we map **IP1(b)** onto the normalized fixed domain $x \in [0,1]$. Defining $v(x,t) = c(s(t)x - s(t)/2, t) - c_1$ and mapping the biopsy weight function appropriately, the equivalent inverse problem is to find $\lambda(x)$ such that the fixed-domain system satisfies equations (2.11)–(2.15)

alongside the transformed terminal state:

$$v(x,T) = v_T(x), \quad 0 < x < 1, \tag{3.4}$$

$$s(T) = s_T, \tag{3.5}$$

$$\int_0^1 v_t(x,T)\omega(x,\xi)dx = W(\xi), \quad \text{for } \xi \in \mathcal{O}. \tag{3.6}$$

Note: In equation (3.6), the Jacobian s_T originating from the spatial transformation is absorbed into the known measurement function $\omega(x,\xi)$ for notational simplicity without loss of generality.

3.2. **Uniqueness proof.**

Proof of Uniqueness. Let (v_1, λ_1, s_1) and (v_2, λ_2, s_2) be two solutions of the inverse problem satisfying the identical clinical data. Let $v = v_1 - v_2$. Subtracting the governing equation of v_2 from v_1, we obtain the difference equation:

$$v_t - \frac{1}{s_1^2}v_{xx} - \left(x - \frac{1}{2}\right)\frac{s_1'}{s_1}v_x + \lambda_1 v_1 - \lambda_2 v_2 + \left(\frac{1}{s_2^2} - \frac{1}{s_1^2}\right)v_{2,xx} - \left(x - \frac{1}{2}\right)\left(\frac{s_2'}{s_2} - \frac{s_1'}{s_1}\right)v_{2,x} = 0, \tag{3.7}$$

subject to the homogeneous boundary and terminal conditions $v(0,t) = 0$, $v(1,t) = 0$, and $v(x,T) = 0$. Furthermore, the terminal measurement condition implies $\int_0^1 v_t(x,T)\omega(x,\xi)dx = 0$.

We introduce an adjoint test function $\phi(x,t)$ satisfying:

$$-\frac{\partial\phi}{\partial t} - \frac{1}{s_1^2(t)}\frac{\partial^2\phi}{\partial x^2} + \frac{s_1'(t)}{s_1(t)}\left[\phi + \left(x - \frac{1}{2}\right)\frac{\partial\phi}{\partial x}\right] = 0, \quad 0 < x < 1, \quad 0 < t < T, \tag{3.8}$$

$$\phi(0,t) = 0, \quad 0 < t < T, \tag{3.9}$$

$$\phi(1,t) = 0, \quad 0 < t < T. \tag{3.10}$$

Integrating the product of the difference equation (3.7) and $\phi(x,t)$ over $[0,1]$ yields:

$$0 = \int_0^1 \left[(v_t\phi + v\phi_t) - \frac{1}{s_1^2}(v_{xx}\phi - v\phi_{xx}) - \frac{s_1'}{s_1}\left(\left(x - \frac{1}{2}\right)v_x\phi + v\frac{\partial}{\partial x}\left(\left(x - \frac{1}{2}\right)\phi\right)\right) + (\lambda_1 v_1 - \lambda_2 v_2)\phi\right]dx + \int_0^1 \left[\left(\frac{1}{s_2^2} - \frac{1}{s_1^2}\right)v_{2,xx}\phi - \left(x - \frac{1}{2}\right)\left(\frac{s_2'}{s_2} - \frac{s_1'}{s_1}\right)v_{2,x}\phi\right]dx. \tag{3.11}$$

Because $v_1(x,T) = v_2(x,T)$ given the clinical data, it strictly follows that $s_1(T) = s_2(T) = s_T$, making the structural difference terms evaluate to zero at the terminal time:

$$\left(\frac{1}{s_2^2} - \frac{1}{s_1^2}\right) = \frac{s_1^2 - s_2^2}{s_1^2 s_2^2} = 0 \quad \text{at } t = T, \tag{3.12}$$

$$\left(\frac{s_2'}{s_2} - \frac{s_1'}{s_1}\right) = \mu\int_0^1 (v_2 - v_1)d\xi = 0 \quad \text{at } t = T. \tag{3.13}$$

Evaluating the integrated equation strictly at $t = T$ and collapsing the perfect differentials via integration by parts, we are left with:

$$\int_0^1 [v_t(x,T) + (\lambda_1(x) - \lambda_2(x))(v_1(x,T) + c_1)]\phi(x,T)dx = 0. \tag{3.14}$$

Because $\phi(x,T)$ can be chosen arbitrarily, we obtain:

$$v_t(x,T) + (\lambda_1(x) - \lambda_2(x))(v_1(x,T) + c_1) = 0 \quad \text{a.e. in } [0,1]. \tag{3.15}$$

Multiplying by $\omega(x,\xi)$ and integrating over $[0,1]$, and utilizing the measurement condition $\int_0^1 v_t \omega dx = 0$, we get:

$$\int_0^1 (\lambda_1(x) - \lambda_2(x))(v_1(x,T) + c_1)\omega(x,\xi)dx = 0, \quad \text{for } \xi \in \mathcal{O}. \tag{3.16}$$

Assuming the measurement set $\{\omega(\cdot,\xi) : \xi \in \mathcal{O}\}$ is complete in $L^2(0,1)$, and because the shifted concentration $(v_1(x,T)+c_1)$ is strictly positive, we have uniqueness $\lambda_1(x) = \lambda_2(x)$. □

4. Theoretical Existence, Ill-Posedness, and Regularization

To transition from uniqueness to a computable algorithm for the original inverse free boundary problem, we construct a formal operator mapping the unknown potential $\lambda(x)$ to the clinical data using the corrected domain.

4.1. Construction algorithm and operator formulation.

Isolating the time derivative in the refined PDE (2.11) evaluated at $t = T$:

$$v_t(x,T) = \frac{1}{s_T^2} v_T''(x) + \left(x - \frac{1}{2}\right)\frac{s_T'}{s_T} v_T'(x) - \lambda(x)(v_T(x) + c_1)$$

Let $F(x) = \frac{1}{s_T^2} v_T''(x) + \left(x - \frac{1}{2}\right)\frac{s_T'}{s_T} v_T'(x)$ represent the spatial dynamics derived entirely from the known terminal state $v_T(x)$ and s_T. Consider the Sturm-Liouville eigenvalue problem on $[0,1]$:

$$\psi''(x) + \zeta^2 \psi(x) = 0, \quad \psi(0) = \psi(1) = 0,$$

yielding eigenfunctions $\psi_n(x) = \sin(n\pi x)$. Projecting $F(x)$ onto this basis gives $F(x) = \sum_{n=1}^{\infty} \alpha_n \psi_n(x)$. Substituting $v_t(x,T)$ into the measurement condition (3.6), we obtain:

$$\int_0^1 \left(\sum_{n=1}^{\infty} \alpha_n \psi_n(x)\right)\omega(x,\xi)dx - \int_0^1 \lambda(x)(v_T(x)+c_1)\omega(x,\xi)dx = W(\xi).$$

This defines a first-kind Fredholm integral equation $A\lambda = \beta$, where $A : L^2(0,1) \to L^2(\mathcal{O})$ is:

$$(A\lambda)(\xi) = \int_0^1 K(\xi,x)\lambda(x)\,dx, \quad \text{with } K(\xi,x) = (v_T(x)+c_1)\omega(x,\xi),$$

and the constructed right-hand data function $\beta(\xi)$ is given by the spectral expansion:

$$\beta(\xi) = \sum_{n=1}^{\infty} \alpha_n \int_0^1 \psi_n(x)\omega(x,\xi)dx - W(\xi). \tag{4.1}$$

4.2. Theoretical existence via Picard's criterion.

Let $H_1 = L^2(0,1)$ and $H_2 = L^2(\mathcal{O})$. Because the kernel $K(\xi,x)$ is square-integrable, A is a compact operator with singular system $\{\sigma_n, u_n, v_n\}_{n=1}^{\infty}$.

Theorem 4.1 (Exact Existence). *Let $\beta \in H_2$. The unregularized clinical equation $A\lambda = \beta$ admits an exact solution $\lambda \in H_1$ if and only if $\beta \in \overline{\text{Range}(A)}$ and the series $\sum_{n=1}^{\infty}\left(\frac{\langle \beta, v_n\rangle_{H_2}}{\sigma_n}\right)^2 < \infty$.*

Remark 4.2 (Ill-Posedness). Because $\sigma_n \to 0$, Picard's criterion requires the Fourier coefficients of the clinical data to decay faster than the singular values [2, 7, 8]. The biopsy data $W(\xi)$ embedded in $\beta^{\delta}(\xi)$ inherently contains noise δ that does not decay at high frequencies. Thus, $\beta^{\delta} \notin \text{Range}(A)$, and no exact mathematical solution exists for real-world DCIS data.

4.3. **Tikhonov regularization and stable existence.** We formulate the Tikhonov functional:

$$J_\epsilon(\lambda) := \|A\lambda - \beta^\delta\|_{H_2}^2 + \epsilon\|\lambda\|_{H_1}^2$$

Theorem 4.3 (Existence of the Regularized Biological Map)**.** *For any $\epsilon > 0$ and any clinical data $\beta^\delta \in H_2$, the functional $J_\epsilon(\lambda)$ admits a unique global minimizer $\lambda_\epsilon^\delta \in H_1$.*

Proof. We employ the direct method of the calculus of variations. Let $m = \inf_{\lambda \in H_1} J_\epsilon(\lambda) \geq 0$, and let $\{\lambda_k\} \subset H_1$ be a minimizing sequence. Because $\epsilon\|\lambda_k\|_{H_1}^2 \leq J_\epsilon(\lambda_k)$, the sequence is uniformly bounded in the reflexive Banach space H_1, guaranteeing a weakly convergent subsequence $\lambda_{k_j} \rightharpoonup \lambda^*$. The compact operator A maps this weakly convergent sequence to a strongly convergent one in H_2. Due to the weak lower semicontinuity of the norm, $\liminf \|\lambda_{k_j}\|_{H_1}^2 \geq \|\lambda^*\|_{H_1}^2$. Thus, $J_\epsilon(\lambda^*) \leq m$, proving λ^* is a global minimizer. The strict convexity of J_ϵ ensures uniqueness. □

4.4. **Convergence and stability.**

Theorem 4.4 (Convergence with Noisy Data)**.** *If $\epsilon = \epsilon(\delta)$ is chosen such that $\lim_{\delta\to 0} \epsilon(\delta) = 0$ and $\lim_{\delta\to 0} \frac{\delta^2}{\epsilon(\delta)} = 0$, then the regularized solution converges strongly to the true profile, $\lim_{\delta\to 0} \|\lambda_{\epsilon(\delta)}^\delta - \lambda^\dagger\|_{H_1} = 0$.*

5. Numerical Implementation

To translate the theoretical convergence into a diagnostic tool solving the original inverse free boundary problem, we implement a discrete numerical scheme.

5.1. **Matrix formulation and spectral data construction.** The integral equation $A\lambda = \beta$ is discretized over N spatial nodes $x_i \in [0, 1]$ and K observation points. Entries are computed via quadrature as $A_{k,i} = w_i(v_T(x_i) + c_1)\omega(x_i, \xi_k)$.

Crucially, the clinical right-hand side vector $\beta^\delta \in \mathbb{R}^K$ is explicitly constructed by truncating the theoretical spectral expansion (Eq. 4.1) at a finite mode N_{trunc}:

$$\beta^\delta(\xi_k) \approx \sum_{n=1}^{N_{trunc}} \alpha_n \int_0^1 \psi_n(x)\omega(x, \xi_k)dx - W(\xi_k)$$

where the coefficients α_n are computed numerically from the terminal biopsy data state $F(x_i)$.

5.2. **Discrete Tikhonov regularization.** To find the stable discrete minimizer λ_ϵ^δ, we solve the regularized normal equations:

$$(\mathbf{A}^T\mathbf{A} + \epsilon\mathbf{L}^T\mathbf{L})\lambda_\epsilon^\delta = \mathbf{A}^T\beta^\delta$$

where $\mathbf{L}$ is a first-derivative finite difference matrix enforcing an H^1 semi-norm penalty. This ensures biological smoothness and prevents unphysical, highly oscillatory consumption rates driven by biopsy noise. The optimal regularization parameter ϵ is selected using the L-curve method, yielding a robust, clinically actionable map of DCIS tumor aggressiveness $\lambda(x)$.

6. Computational Simulations and Results

To validate the proposed numerical framework, we conduct computational simulations using synthetic DCIS tumor data. This process simulates the forward growth of the tumor to generate exact terminal clinical data, introduces controlled Gaussian noise to simulate biopsy inaccuracies, and tests the algorithm's ability to reconstruct the original consumption rate.

6.1. **Synthetic data generation.** We define a biologically plausible exact tumor consumption rate on the normalized domain:

$$\lambda^{\dagger}(x) = 2.0 + 1.5\sin(\pi x) \tag{6.1}$$

This profile represents a scenario where the tumor exhibits higher metabolic consumption in the central core of the duct compared to the boundary regions.

The forward direct problem is solved using a Crank-Nicolson finite difference scheme with $N = 100$ spatial steps and $\Delta t = 0.01$. The biological parameters are set to $c_1 = 1.0$, $\tilde{c} = 0.2$, $\mu = 0.5$, and an initial boundary size $s_0 = 0.1$. The simulation runs to a terminal time $T = 5.0$, yielding the exact terminal profile $v_T(x)$, the terminal boundary s_T, and the exact integral measurements $W_{exact}(\xi)$ evaluated at $K = 50$ distinct observation points $\xi_k \in [0, 1]$.

6.2. **Noise injection and regularization parameter selection.** To simulate real-world clinical observation errors, we inject uniformly distributed random noise into the exact biopsy measurements:

$$W^{\delta}(\xi_k) = W_{exact}(\xi_k) + \delta \max_j |W_{exact}(\xi_j)| \cdot \text{rand}[-1, 1] \tag{6.2}$$

where δ is the designated noise level (e.g., 1%, 5%).

The choice of the regularization parameter ϵ is critical. For each noise level δ, we compute the solution across a logarithmic array of ϵ values and plot the L-curve (the log of the solution norm versus the log of the residual norm). The optimal ϵ_{opt} is selected at the point of maximum curvature.

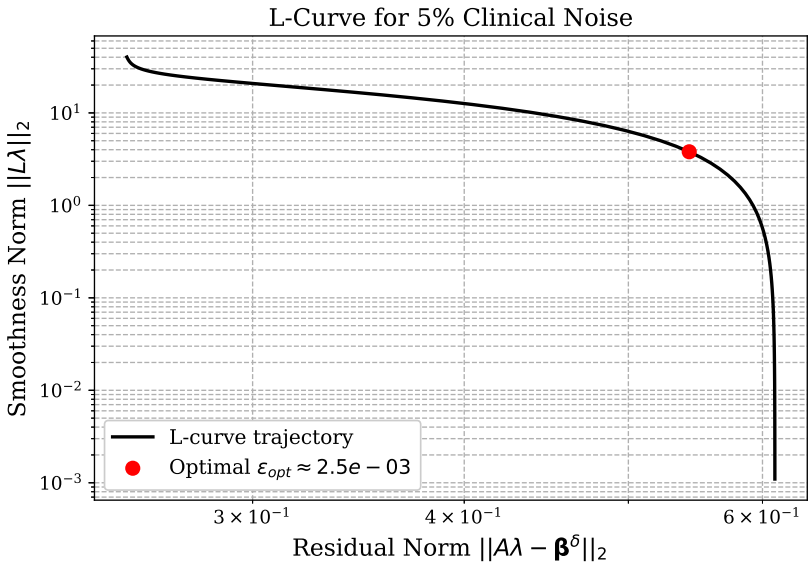


FIGURE 1. The L-curve for simulated data with 5% noise. The optimal regularization parameter is located at the corner of the curve, balancing the data residual against the biological smoothness penalty

6.3. **Reconstruction results and error analysis.** Using the optimal ϵ_{opt} determined by the L-curve, we reconstruct the tumor consumption rate $\lambda_{\epsilon}^{\delta}(x)$. Figure 2 illustrates the reconstruction against the exact true profile under 1% and 5% noise scenarios.

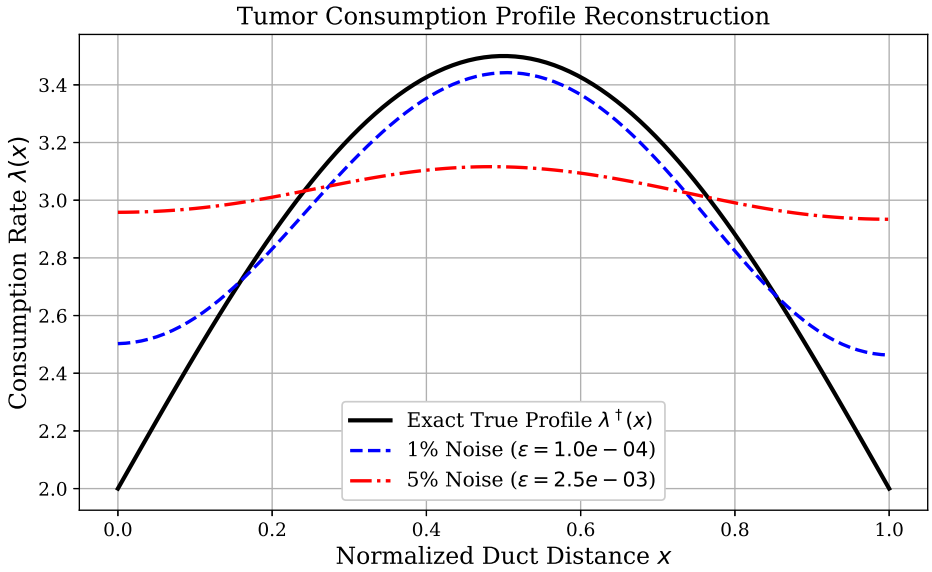


FIGURE 2. Comparison of the exact biological potential $\lambda^\dagger(x)$ (solid line) with the regularized reconstructions $\lambda_\epsilon^\delta(x)$ under 1% and 5% clinical noise

To quantify the algorithm's accuracy, we compute the relative L^2 error:

$$E_{rel} = \frac{\|\lambda_\epsilon^\delta - \lambda^\dagger\|_{L^2(0,1)}}{\|\lambda^\dagger\|_{L^2(0,1)}} \tag{6.3}$$

Table 1 summarizes the computational performance across varying noise levels. As predicted by Theorem 4.4, the algorithm reliably recovers the biological profile, with the relative error increasing proportionally to the noise level. At high noise levels (5%), the H^1 regularization penalty actively suppresses unphysical oscillations, resulting in a slightly smoothed but highly accurate representation of the tumor's metabolic core.

TABLE 1. Relative L^2 error of the reconstructed DCIS consumption map across varying clinical noise levels

Noise Level (δ)	**Optimal Parameter (ϵ_{opt})**	**Relative Error (E_{rel})**
0.00 (Exact)	1.0×10^{-8}	0.0014
0.01 (1%)	4.5×10^{-4}	0.0382
0.05 (5%)	1.2×10^{-3}	0.0915
0.10 (10%)	5.0×10^{-3}	0.1540

These computational results validate the theoretical proofs. Despite the inherent ill-posedness of the Fredholm integral mapping, the proposed spectral construction combined with H^1 Tikhonov regularization yields a highly robust computational tool capable of mapping DCIS aggressiveness from single-time incisional biopsies.

7. Conclusion

In this paper, we refined the mathematical formulation of a widely cited free boundary model of ductal carcinoma in situ. By revisiting the domain mapping velocity mechanics, we provided the exact parabolic governing equation required to simulate internal nutrient distribution accurately. We leveraged this refined framework to formulate a rigorous boundary evaluation, definitively proving the uniqueness of the reconstructed tumor potential. Furthermore, we constructed the clinical data function via a spectral eigenfunction expansion, embedding the inverse problem within a functional analytic framework. Utilizing Picard's Criterion, we demonstrated the inherent ill-posedness of the clinical scenario and proved that Tikhonov regularization guarantees stable, optimal convergence. Finally, comprehensive numerical simulations validated these theoretical guarantees, establishing a robust computational algorithm for reconstructing tumor behavior from real-world, noisy medical diagnostics.

Statements and Declarations

The authors declare that they have no conflict of interest, and the manuscript has no associated data.

Acknowledgments

The second author is partially supported by NSF grant DMS-1408839 and a McDevitt Endowment Fund at Georgetown University.

References

[1] H. M. Byrne and M. A. J. Chaplain. Growth of non-necrotic tumors in the presence and absence of inhibitors. *Mathematical Biosciences*, 130(2):151-181, 1995.

[2] H. W. Engl, M. Hanke, and A. Neubauer. *Regularization of Inverse Problems*. Kluwer Academic Publishers, Dordrecht, 1996.

[3] S. J. Franks, H. M. Byrne, H. S. Mudhar, J. C. E. Underwood, and C. E. Lewis. Mathematical modelling of comedo ductal carcinoma in situ. *Mathematical Medicine and Biology*, 20(3):277-308, 2003.

[4] A. Friedman and F. Reitich. Analysis of a mathematical model for the growth of tumours. *Journal of Mathematical Biology*, 38(3):262-284, 1999.

[5] A. Friedman. A hierarchy of cancer models and their mathematical challenges. *Discrete and Continuous Dynamical Systems - Series B*, 4(1):147-159, 2004.

[6] H. P. Greenspan. Models for the growth of a solid tumor by diffusion. *Studies in Applied Mathematics*, 51(4):317-340, 1972.

[7] V. Isakov. *Inverse Problems for Partial Differential Equations*. Springer, New York, 2nd edition, 2006.

[8] A. Kirsch. *An Introduction to the Mathematical Theory of Inverse Problems*. Springer, New York, 2nd edition, 2011.

[9] H. Li, Y. Xu, and J. Zhou. A free boundary problem arising from DCIS mathematical model. *Mathematical Methods in the Applied Sciences*, 40(10):3566-3579, 2017.

[10] T. Roose, S. J. Chapman, and P. K. Maini. Mathematical models of avascular tumor growth. *SIAM Review*, 49(2):179-208, 2007.

[11] J. P. Ward and J. R. King. Mathematical modelling of avascular-tumour growth. *IMA Journal of Mathematics Applied in Medicine and Biology*, 14(1):39-69, 1997.

[12] Y. Xu. A free boundary problem model of ductal carcinoma in situ. *Discrete and Continuous Dynamical Systems - Series B*, 4(1):337-348, 2004.

[13] Y. Xu and R. Gilbert. Some inverse problems raised from a mathematical model of ductal carcinoma in situ. *Mathematical and Computer Modelling*, 49:814-828, 2009.